Research Article

Lan Anh Thi Nguyen, Bay Van Mai, Din Van Nguyen, Ngoc Quyen Thi Nguyen, Vuong Van Pham, Thong Le Minh Pham, and Hai Tu Le*

Green synthesis of silver nanoparticles using *Callisia fragrans* leaf extract and its anticancer activity against MCF-7, HepG2, KB, LU-1, and MKN-7 cell lines

https://doi.org/10.1515/gps-2023-0024
received February 10, 2023; accepted April 20, 2023

Abstract: This article presents a simple, eco-friendly, and green method for the synthesis of silver nanoparticles (AgNPs) from $AgNO_3$ solution utilizing an aqueous extract of *Callisia fragrans* leaf. The effects of *C. fragrans* leaf extraction conditions were evaluated. Parameters affecting the synthesis of AgNPs, such as the volume of extract, pH, temperature, and reaction time were investigated and optimized. The obtained AgNPs were analyzed by UV–Vis spectroscopy, X-ray diffraction pattern, energy-dispersive X-ray spectroscopy, field emission scanning electron microscopy, transmission electron microscopy (TEM), dynamic light scattering (DLS), and FTIR techniques. TEM and DLS analyses have shown that the synthesized AgNPs were predominantly spherical in shape with an average size of 48 nm. The zeta potential of the colloidal solution of AgNPs is –27 mV, indicating the dispersion ability of AgNPs. The results of GC–MS and FTIR analyses show the presence of biomolecules in the aqueous extract of *C. fragrans* leaf that acts as reducing and capping agents for the biosynthesis of AgNPs. The synthesized AgNPs demonstrate anticancer activity against MCF-7, HepG2, KB, LU-1, and MKN-7 cell lines, with inhibitory concentrations at 50% (IC_{50} values) of 2.41, 2.31, 2.65, 3.26, and 2.40 $\mu g \cdot mL^{-1}$, respectively. The obtained results in the study show that the biosynthesized AgNP from *C. fragrans* leaf extract can be further exploited as a potential candidate for anticancer agents.

Keywords: biosynthesis, plant extract, UV–Vis absorption spectrum, surface plasmon, nanoparticles

1 Introduction

Nanotechnology is one of the most active fields of research in materials science. Nanoparticles have completely new and improved properties based on specific characteristics such as their size, distribution, and morphology. The development of reliable, eco-friendly processes for the synthesis of nanomaterials is an important aspect of nanotechnology, which is called green nanotechnology. Nanoparticles of metals are well recognized to have significant applications in electronics, magnetic, optoelectronics, and information storage [1]. In medicine, metallic nanomaterial like gold, silver, iron, copper, tellurium, and zinc oxide nanoparticles reported to play a powerful role in antioxidant, antibacterial, antifungal, and anticancer [2–5].

Among the various metal nanoparticles, silver nanoparticles (AgNPs) have found applications in products ranging from food, medicine, and consumer products to washing machines [6–8]. Moreover, AgNPs have recently attracted attention as the anticancer agent against the cell lines such as MCF-7, Hep2, HepG2, HCT-116 colon, HT29, HELA, Caco2, and A549 [9–19]. The main mechanisms of AgNPs in cancer therapy also suggest that AgNPs induce cell death through reactive oxygen species (ROS) generation, activation of caspase 3, and DNA fragmentation [20].

AgNPs are typically synthesized by different methods such as physical and chemical methods. The physical methods include laser ablation [21], spark discharging [22], and pyrolysis [23]. The chemical methods are electrochemical reduction

* **Corresponding author: Hai Tu Le,** Department of Chemistry, The University of Da Nang – University of Science and Education, Da Nang 550000, Vietnam, e-mail: lthai@ued.udn.vn
Lan Anh Thi Nguyen, Bay Van Mai, Din Van Nguyen, Ngoc Quyen Thi Nguyen: Department of Chemistry, The University of Da Nang – University of Science and Education, Da Nang 550000, Vietnam
Vuong Van Pham: C17 Hospital, Da Nang 550000, Vietnam
Thong Le Minh Pham: Institute of Research and Development, Duy Tan University, Da Nang 550000, Vietnam

[24], chemical reduction [25], solution irradiation [26], etc. The major process involved in chemical synthesis is the reduction of Ag^+ ions to AgNPs.

The major disadvantage in the physical method is the low yield and complex instruments. The disadvantage in the chemical method is the use of toxic solvent and expensive stabilizing agents are also required to prevent the aggregation of nanoparticles to make them physiologically compatible, which may pose potential environmental and biological risks [27]. Thus, the development of the green methods for the synthesis of AgNPs is of great scientific interest. The main advantages of biological method for AgNPs synthesis are its simplicity, low cost, non-toxicity, and ease of upscaling. Several biological systems including bacterial [28], fungi [29], algae [30], yeast [31], chitosan [32], and particularly plant extracts [33–42] have been used in the synthesis of AgNPs.

The synthesis of AgNPs employing reducing agents from plant extracts is based on the redox reactions of biological compounds in the extracts such as flavonoids, terpenoids, polyphenols, alkaloids, and sugars with Ag^+ [43]. The functional groups in phytochemical compounds, whose redox potential is less than that of silver ion can reduce silver cation to silver atoms, which then aggregate to form AgNPs. The biological compounds are adsorbed on the surfaces of newly-synthesized AgNPs, encapsulating them to prevent agglomeration and stabilize the AgNPs colloidal solution. The synthesis of AgNPs using plant extracts does not use any harmful chemicals, and the applicability of AgNPs colloidal solutions is becoming increasingly promising, thanks to the binding of bioactive compounds in plant extracts to the surfaces of AgNPs. The presence of substances extracted from herbal plants on the surface of AgNPs has significantly increased the application of AgNPs in medicine. In addition, the green synthesis of AgNPs employing plant extracts can be carried out under simple conditions. The major limitation of the synthesis of nanoparticles using plants is the long hours required for the synthesis, and the formation of polydisperse mixture of nanoparticles.

Callisia fragrans is an herbaceous plant with small white fragrant flowers and waxy leaves, which can be found widely in Vietnam (its Vietnamese name is Luoc Vang). In Vietnam *C. fragrans* leaves have been used in traditional medicines for treating skin diseases, burns, and joint disorders. *C. fragrans* leaves contain biologically active compounds such as flavonoids, neutral glycol- and phospholipids, and fatty acids [44,45]. Accordingly, *C. fragrans* is considered as an antiviral and antibacterial drug [46].

In this study, we have developed a green method for the synthesis of AgNPs using *C. fragrans* leaf aqueous extracts which have been demonstrated as a facile, cheap, and environmentally friendly method. The anticancer activities of the synthesized AgNPs were also investigated.

2 Materials and methods

2.1 Materials

Silver nitrate ($AgNO_3$), sulfuric acid (H_2SO_4), sodium hydroxide (NaOH), *n*-hexane (C_6H_{14}), chloroform ($CHCl_3$), ethyl acetate ($CH_3COOC_2H_5$), and ethanol (C_2H_5OH) were purchased from Merck chemical company (Germany). Fresh *C. fragrans* leaves were collected from various locations in Da Nang City, Vietnam. All aqueous solutions were made using double-distilled water.

The cell lines of human breast carcinoma (MCF-7), human lung carcinoma (Lu-1), human hepatocellular carcinoma (HepG2), human carcinoma in the mouth (KB), and human gastric carcinoma (MKN-7) were obtained from Long-Island University, USA and Milan University, Italia.

2.2 Preparation of leaf extract

The leaves were washed thoroughly with double-distilled water and then dried by air. Predetermined masses of leaves were cut into fine pieces. The influences of the ratio of *C. fragrans* leaf mass/water volume, extraction time, and extraction temperature to the efficacy of *C. fragrans* leaf extraction were investigated. After the boiling process, the extract was filtered through Whatman No. 1 filter paper to obtain an aqueous extract, which was directly used in the synthesis of AgNPs or stored at 4°C for further experiments.

2.3 Phytochemical screening of aqueous extract of *C. fragrans* leaf

The aqueous extract of *C. fragrans* leaf was screened for the presence of phytochemicals like terpenoids, flavonoids, alkaloids, tannins, and saponins using standard color tests [47].

2.4 Chemical constituent of aqueous extract of *C. fragrans* leaf

The aqueous extract of *C. fragrans* leaf is extracted by liquid–liquid method with *n*-hexane, chloroform, and ethyl acetate solvents to, respectively, yield *n*-hexane extract, chloroform extract, and ethyl acetate extract. The remaining aqueous extract were concentrated and dissolved in ethanol to obtain ethanol extract. These extracts are subjected to GC–MS analysis using GC–MS 7890B-5977B – Agilent. A capillary column HP-5MS (30 m × 0.25 mm i.d. and 0.25 µm film thickness) was used for separating the components. Helium gas was used as the carrier gas with a flow rate of 1.1 mL·min^{-1}. The temperature of the oven varied from 40°C to 280°C at a rate of 5 min^{-1} with a holding time of 1–10 min. The injector temperature was 270°C, and the injection volume was 1.0 µL. The identification of components of the extracts was based on a comparison between Kovat's retention indices and mass spectra that corresponded with data (Adam, 1989) and mass spectra libraries (National Institute of Standards and Technology 98).

2.5 Synthesis of AgNPs

For the synthesis of AgNPs, a definite volume of leaf extract was mixed with a volume of 1 mM $AgNO_3$ in 100 mL Erlenmeyer flasks. The reaction was carried out by placing the flasks in a water bath for a specified synthesis time and temperature. The color change in the colloidal solutions occurred indicating the formation of AgNPs. The influence of some factors such as the volume ratio of *C. fragrans* leaf extract/$AgNO_3$ solution, pH, reaction temperature, and reaction time for the synthesis of AgNPs was investigated.

2.6 Characterization of AgNPs

The formation of AgNPs was characterized by UV–visible (UV–Vis) spectroscopy. The synthesized AgNPs solution was diluted ten times and measured using the UV–Vis spectra. The UV–Vis spectra of these samples were measured between 350 and 700 nm on a UV–VIS Perkin Elmer Lambda 365 spectrophotometer operated at a resolution of 1 nm. The samples for electron microscopy were gold coated (JEOL, Model No. JFC-1600), and images were obtained by scanning electron microscope (ZEISS EVO-MA 10, Oberkochen, Germany). The samples for transmission electron microscopy (TEM) analysis were prepared by drop coating biologically synthesized AgNPs solution onto carbon-coated copper TEM grids. TEM measurements and energy-dispersive X-ray spectroscopy (EDX) analysis were carried out using HRTEM Tecnai G2 F20. Crystal phase identification of AgNPs was characterized by powder X-ray diffraction using a Panlytical X Pert PRO Diffractometer. The diffracted intensities were recorded from 10° to 70° 2θ angles. The zeta potential and hydrodynamic size were calculated using HORIBA SZ-100. FTIR was carried out with JASCO FT/IR-6800 to investigate the type of functional groups involved in the reduction and capping of AgNPs.

2.7 Evaluation of *in vitro* cytotoxic activity of the AgNPs on cancer cell lines

The *in vitro* cytotoxicity of AgNPs was determined using human breast carcinoma (MCF-7), human lung carcinoma (Lu-1), human hepatocellular carcinoma (HepG2), human carcinoma in the mouth (KB), and human gastric carcinoma (MKN-7) cell lines. These tests were performed by the Institute of Biotechnology – Vietnam Academy of Science and Technology according to the sulforhodamine B (SRB) assay. The test was carried out to determine the total cellular protein content based on the optical density (OD) measured when the protein composition of the cells was stained with SRB. The measured OD value is directly proportional to the amount of SRB bonded to the protein molecule, so the more the cells (the more protein) the larger the OD value. The test was carried out under the following specific conditions: trypsinizing experimental cells to separate cells and counting in a counting chamber to adjust the density to suit the experiment. Proceed to put 190 µL of cells in 96-well plate for testing. The prepared sample (10 µL) was introduced into the wells of the cell-prepared test a 96-well plate. Wells without reagent but contained cancer cells (190 µL) + DMSO 1% (10 µL) were used as day 0 control. After 1 h, cells were fixed with trichloroacetic acid (TCA) 20% in day 0 control wells. Cells were then incubated in the incubator for 72 h. After 72 h, the cells were fixed with TCA for 1 h, stained with SRB for 30 min at 37°C, washed three times with acetic acid, and then dried at room temperature. Unbuffered Tris base of 10 mM was used to dissolve the amount of SRB, then the mixture was shook gently for 10 min. The OD result was determined at 540 nm on an ELISA Plate Reader (Biotek). The inhibition percentage of cell growth in the presence of reagents is calculated by the following equation:

$$\% \text{ Inhibition} = 100\% - \frac{\text{OD (sample)} - \text{OD (day0)}}{\text{OD (DMSO)} - \text{OD (day0)}} \quad (1)$$

Ellipticine at concentrations of 10, 2, 0.4, and 0.08 μg·mL^{-1} was used as the reference control; 1% DMSO was used as a negative control (final concentration in the test well is 0.05%). All experiments were performed in triplicate and the results were expressed as the mean ± standard deviation. The IC_{50} value (concentration that inhibits 50% of growth) was determined using Table Curve 2Dv4 computer software.

3 Results and discussion

3.1 Optimization for the extraction of *C. fragrans* leaf

The influence of some factors on the extraction process of phytochemical compounds present in *C. fragrans* leaf was studied. The obtained extract of *C. fragrans* leaves (10 mL) was mixed with 30 mL of 1 mM $AgNO_3$ solution in Erlenmeyer flasks. The flask was kept in a water bath at 70°C for 60 min. A change in the color was observed indicating the formation of AgNPs.

3.1.1 Effect of solid/liquid ratio

The effect of the ratio of *C. fragrans* leaf weight/distilled water volume on the formation of AgNPs was studied with experimental parameters as follows. The time of extraction was 60 min and the extraction temperature was 60°C. The ratio of *C. fragrans* leaf weight/distilled water volume varied from 5 g·100 mL^{-1} to 10 g·100 mL^{-1}, 15 g·100 mL^{-1}, 20 g·100 mL^{-1}, and 25 g·100 mL^{-1}. The UV–Vis spectra (Figure 1) show the effect of *C. fragrans* leaf weight/distilled water volume on the formation of AgPNs from 1 mM $AgNO_3$. Characteristic surface plasmon absorption was observed at 420–460 nm for the brown-colored AgNPs.

The results of Figure 1 show that the intensity of absorption peak increased along with the increase of the ratio of *C. fragrans* leaf from 5 g to 15 g·100 mL^{-1} of distilled water. The reason is that when the *C. fragrans* leaf content increases, the amount of reducing agent is more separated, so the concentration of AgNP is more. However, as the content of *C. fragrans* leaf increased up to 20 g and 25 g·100 mL^{-1}, the intensity of the absorption peak of the obtained AgNPs solution decreased dramatically. This can be explained as follows: when the weight of *C. fragrans* leaf exceeds 15 g, it is possible to create many substances that speed up the creation of AgNPs drastically, the formed particles then coagulate easily into larger-sized version, reducing the intensity of absorption peak [48]. So the optimal solid/liquid ratio is 15 g of *C. fragrans* leaf per 100 mL of distilled water.

3.1.2 Effect of extraction time

The effect of extraction time of *C. fragrans* leaf on the formation of AgNPs was studied under the following

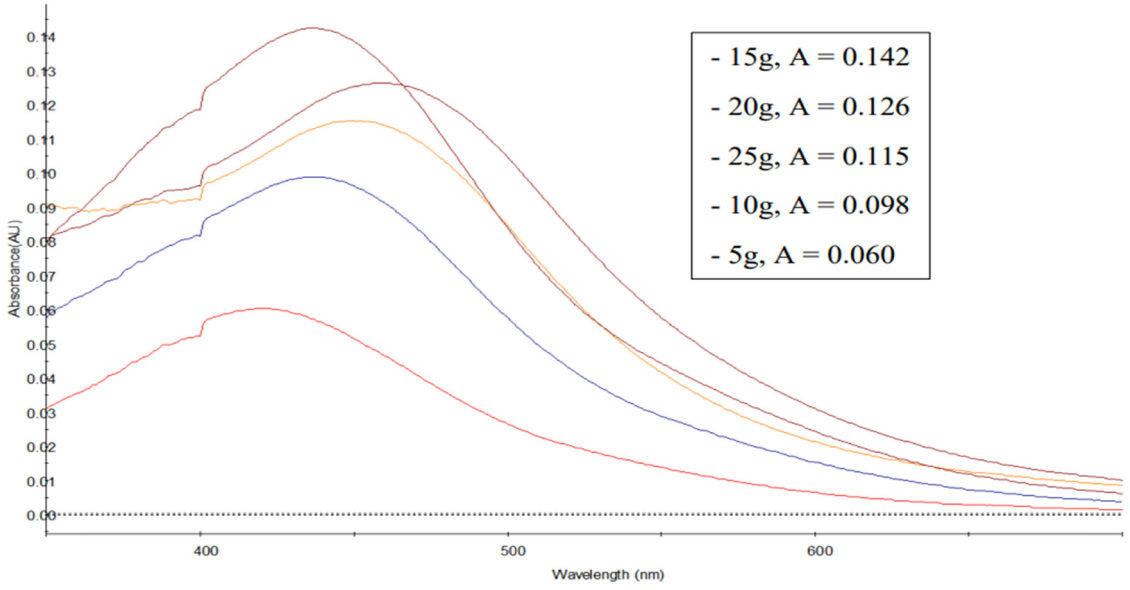

Figure 1: UV–Vis spectra of AgNPs synthesized at the ratio of *C. fragrans* leaf weight/distilled water volume.

conditions: 15 g *C. fragrans* leaf per 100 mL of distilled water, the temperature of extraction was 60°C, and the time for extraction t = 30, 40, 50, 60, 70, 80, and 90 min.

The results of Figure 2 show that the absorption of the synthesized AgNPs solution increased with the increase in the extraction time from 30 to 70 min. As the extraction time was prolonged (80 and 90 min), the intensity of AgNPs absorption decreased considerably. A possible reason for this is that at the extraction time of 70 min, the appropriate amount of reducing agent to reduce the largest amount of silver ions to silver was produced. Beyond this point, substances that are not beneficial to the process of creating AgNPs may be formed or coagulation may occur, reducing the intensity of absorption peak. Thus, the suitable time for the extraction of *C. fragrans* leaf was 70 min.

3.1.3 Effect of extraction temperature

The effect of extraction temperature of *C. fragrans* leaf on the formation of AgNPs was studied with experimental parameters as follows: 15 g of *C. fragrans* leaf per 100 mL of distilled water, an extraction time of 70 min, and the temperature for extraction at 60°C, 70°C, 80°C, 90°C, and boiling temperature.

The obtained results are shown in Figure 3. The intensity of AgNPs absorption increased when extraction temperature increased from 60°C to boiling temperature. Thus, the increase in the intensity of peak can be correlated with an enhancement in the extraction temperature of *C. fragrans* leaf because the higher the extraction temperature, the higher the amount of reducing agent separated. In accordance to above reported results, Ahmadi and coworkers [40] and many others have shown that the preparation of extract by boiling the plant in the water was proved in the synthesis of AgNPs.

In summary, the optimum extraction conditions of phytochemical compounds from *C. fragrans* leaf were found to be 15 g of *C. fragrans* leaf per 100 mL of double distilled water, extraction time of 70 min, and boiling temperature.

3.2 Phytochemical screening of aqueous extract of *C. fragrans* leaf

Standard phytochemical tests were conducted to find the presence of metabolites like terpenoids, flavonoids, alkaloids, tannin, and saponin in the aqueous extract of *C. fragrans* leaf. The results of the phytochemical screening are presented in Table 1.

It is well evident from the table that the aqueous extract was rich in metabolites like terpenoids, flavonoids, tannin, and saponin. These biological compounds are reducing and stabilizing agents for the synthesis of AgNPs [43].

3.3 Chemical constituents of *C. fragrans* leaf aqueous extract by GC/MS

The GC/MS analysis of *C. fragrans* leaf aqueous extract, as given in Table 2, revealed its richness with many

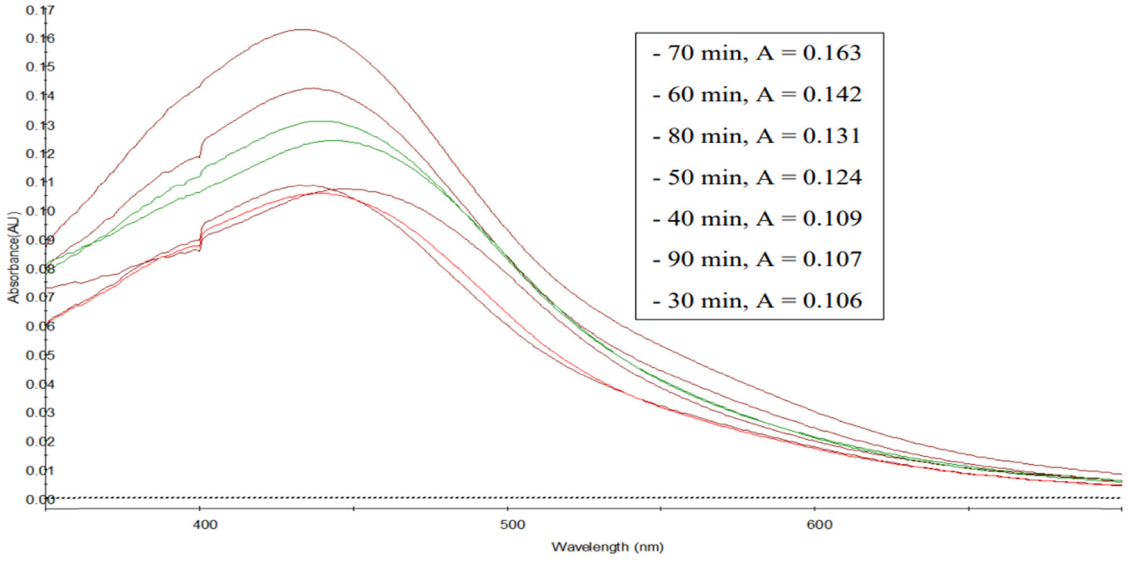

Figure 2: UV–Vis spectra of AgNPs synthesized at various extraction times.

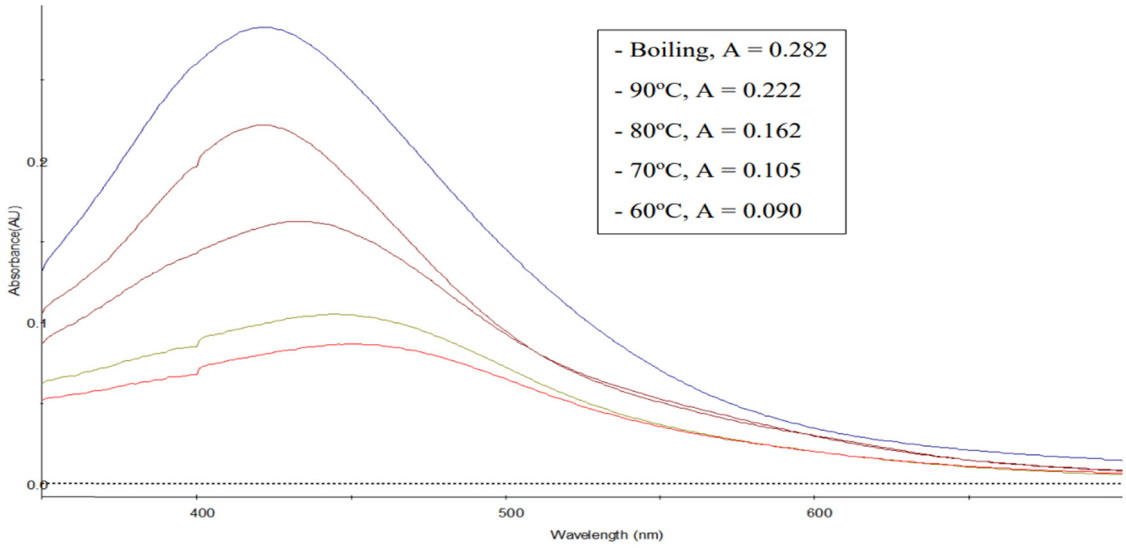

Figure 3: UV–Vis spectra of AgNPs synthesized at various extraction temperatures.

Table 1: Phytochemical screening of aqueous extract of *C. fragrans* leaf

Phytochemical	*C. fragrans* leaf extract
Terpenoids	+
Flavonoids	+
Alkaloids	–
Tannin	+
Saponin	+

– indicates absence, + indicates presence.

bioactive compounds such as beta-amyrin, lupeol, and vitamin E. Beta-amyrin and lupeol are triterpenoids, which are reducing agents for the synthesis of AgNPs and are known to possess potent bioactivities such as anticancer and anti-inflammatory activities.

3.4 Optimization of various parameters to improve the AgNPs synthesis

The effect of mixing ratio (volume of extract per 30 mL of 1 mM $AgNO_3$), temperature, pH, and time, which influence the formation of AgNPs was studied in detail.

3.4.1 Effect of mixing ratio on the formation of AgNPs

To assess the effect of mixing ratio on the formation of AgNPs, 14 samples were tested (from mixing ratio of 1, 2, 3, 4, 5, 6, 7, 8, 9, 10, 11, 12, 13, and 14 mL of extract volume per 30 mL of 1 mM $AgNO_3$ solution volume). The samples after color change were measured by spectroscopy within the wavelength of 350–700 nm (Figure 4).

Table 2: GC–MS analysis of *C. fragrans* leaf aqueous extract

Compound	Chemical formula
Alpha-pinen	$C_{10}H_{16}$
Beta-amyrin	$C_{30}H_{50}O$
Caryophyllene	$C_{15}H_{24}$
Caryophyllene oxide	$C_{15}H_{24}O$
Cetene	$C_{16}H_{32}$
Cyclohexadecane, 1,2-diethyl-	$C_{20}H_{40}$
2,4-Di-*tert*-butylphenol	$C_{14}H_{22}O$
Dihydroactinidiolide	$C_{11}H_{16}O$
Docosyl trifluoroacatate	$C_{24}H_{45}F_3O_2$
Dodecane	$C_{12}H_{26}$
1-Dodecene	$C_{12}H_{24}$
Eicosane	$C_{20}H_{42}$
5-Eicosene, (*E*)-	$C_{20}H_{40}$
Eucalyptol	$C_{10}H_{18}O$
E-15-heptadecenal	$C_{17}H_{32}O$
Hentriacontane	$C_{31}H_{64}$
n-Hexadecanoic acid	$C_{16}H_{32}O_2$
Hexadecanoic acid, ethyl ester	$C_{18}H_{36}O_2$
Humulenen	$C_{15}H_{24}$
Lupeol	$C_{30}H_{50}O$
Nanocos-1-ene	$C_{29}H_{58}$
Octadecanoic acid	$C_{18}H_{36}O_2$
Propane, 1,1,2,3,3-pentachloro	$C_3H_3Cl_3$
Phytol	$C_{20}H_{40}O$
Spathulenol	$C_{15}H_{24}O$
2-Tetradecene, (*E*)-	$C_{14}H_{28}$
Tetracosane	$C_{24}H_{50}$
Tridecane	$C_{13}H_{28}$
Vitamin E	

By changing the mixing ratio in similar environmental conditions, the observed wavelength of maximum peak (λ_{max}) did not change much. However, by increasing the extract volume, the absorption intensity rose and reached its peak at 10 mL of extract per 30 mL of 1 mM $AgNO_3$. This occurred by increasing the extract volume of *C. fragrans* leaf, leading to an increase in the concentration of terpenoids, flavonoids, tannin, saponin, etc., which is responsible for the forming and stabilizing of AgNP. As the extract volume continued to increase (11–15 mL), the absorption intensity decreased. The reason may be that when the extract volume increased, the concentration of the reducing agent in the extract also increased, thus raising the rate of AgNPs generation, thereby leading to an increase in the particle size and reducing the absorption intensity. Thus, the optimal volume of *C. fragrans* leaf extract V = 10 mL per 30 mL of 1 mM $AgNO_3$ solution and the synthesized AgNP solution is not flocculated.

3.4.2 Effect of temperature on the formation of AgNPs

Temperature plays an important role in the synthesis of AgNPs. In order to study the effect of temperature, six containers containing 30 mL of 1 mM $AgNO_3$ together with 10 mL extract were put at six different temperature levels of 50°C, 60°C, 70°C, 80°C, 90°C, and 100°C. The UV–Vis spectra in Figure 5 show the effect of temperature on the formation of AgNPs.

It can be seen from Figure 5 that the synthesis of nanoparticles increases while increasing the reaction temperature from 50°C to 80°C by using the leaf extract of *C. fragrans*. A higher rate of reduction occurred at higher temperature due to the consumption of silver ions in the formation of nuclei of nanoparticles.

As the reaction temperature continued to increase from 90°C to 100°C, the absorption intensity decreased, possibly due to the aggregation of nanoparticles. Mittal et al. [49] have also reported this trend in the biosynthesis of AgNPs.

According to the obtained results, 80°C was selected as the optimum temperature for this study.

3.4.3 Effect of pH level on the formation of AgNPs

pH level plays an important role in AgNPs synthesis [50]. This factor induces the reactivity of leaf extract with silver ions. The influence of pH on the synthesis of AgNPs was evaluated under different pH levels of the reaction mixture by the leaf extract (Figure 6). The obtained results showed that the absorption peak intensity increased gradually with an increase in pH, suggesting that the reduction rate of silver ions increases with the increase in pH. These results are congruent with those reported by other works [51–54]. They attributed this behavior to the possible ionization of the phenolic and tannin compounds present in the mentioned extracts. At low pH, a small

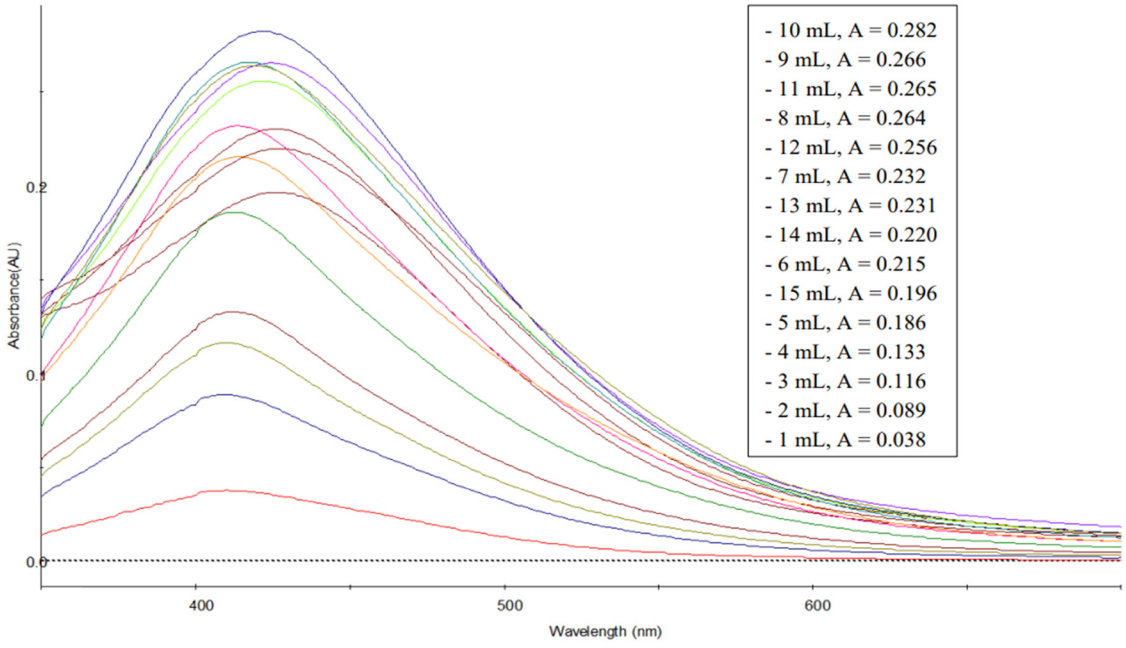

Figure 4: UV–Vis spectra show effect of mixing ratio of extract volume per 30 mL of 1 mM $AgNO_3$ solution in the formation of AgNPs.

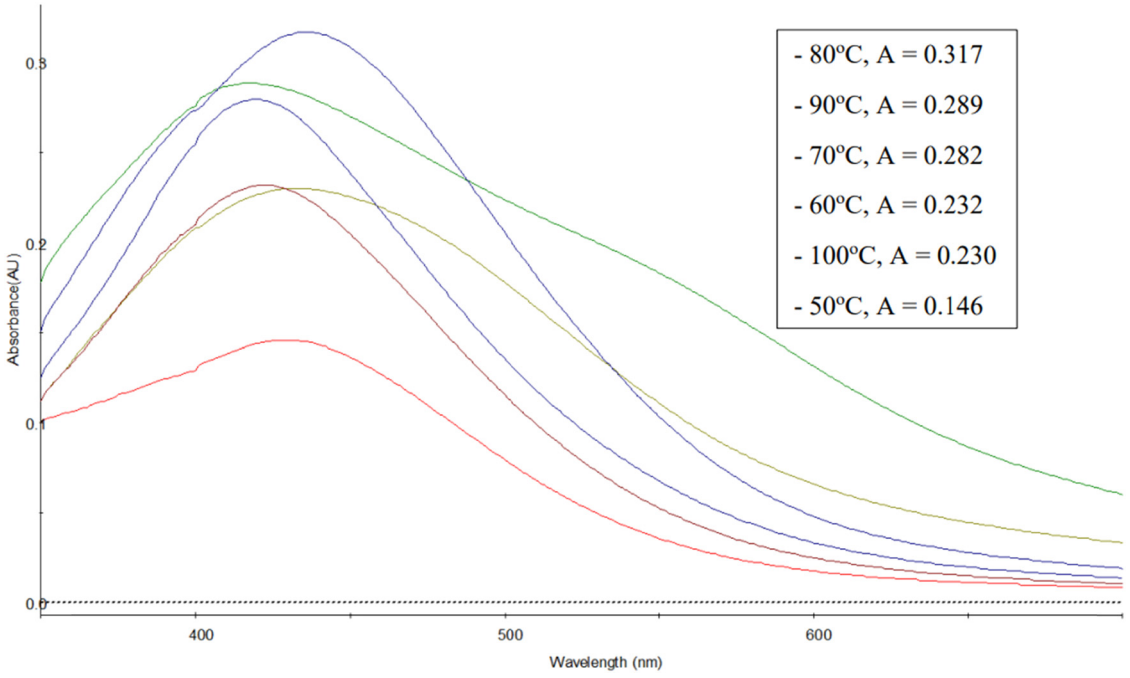

Figure 5: UV–Vis spectra of AgNPs synthesized at the different temperatures.

with broadening SPR band was formed, indicating the formation of a large amount of AgNPs. As the pH level increased from 4.05 to 7.06, the absorption intensity values rose and reached the highest value at pH = 7.06 with a sharp peak. However, at pH = 8.05, 9.06, and 10.04, the amount of AgNPs was formed too fast, leading to coagulation; AgNPs have large size, which reduces the absorption intensity values. Similarly, Sarsar et al. [55] reported that the AgNP synthesis using *P. guajava* leaf extract, pH 7.0 was optimum for the synthesis of the nanoparticles.

3.4.4 Effect of reaction time on the formation of AgNPs

The influence of reaction time on the synthesis of AgNPs was evaluated with the results shown in Figure 7.

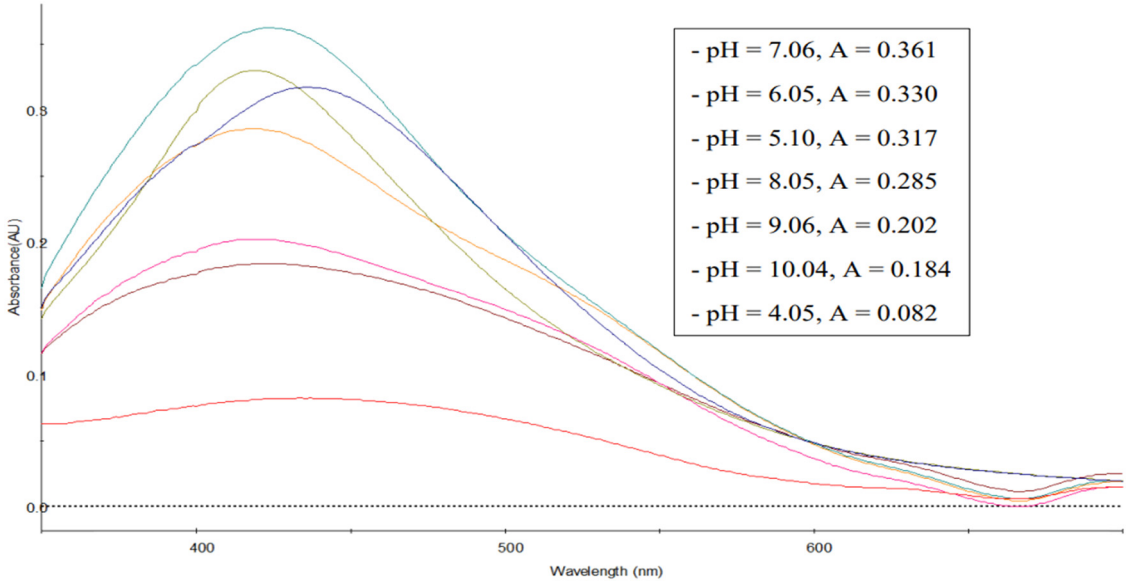

Figure 6: UV–Vis spectra of AgNPs synthesized at various pH.

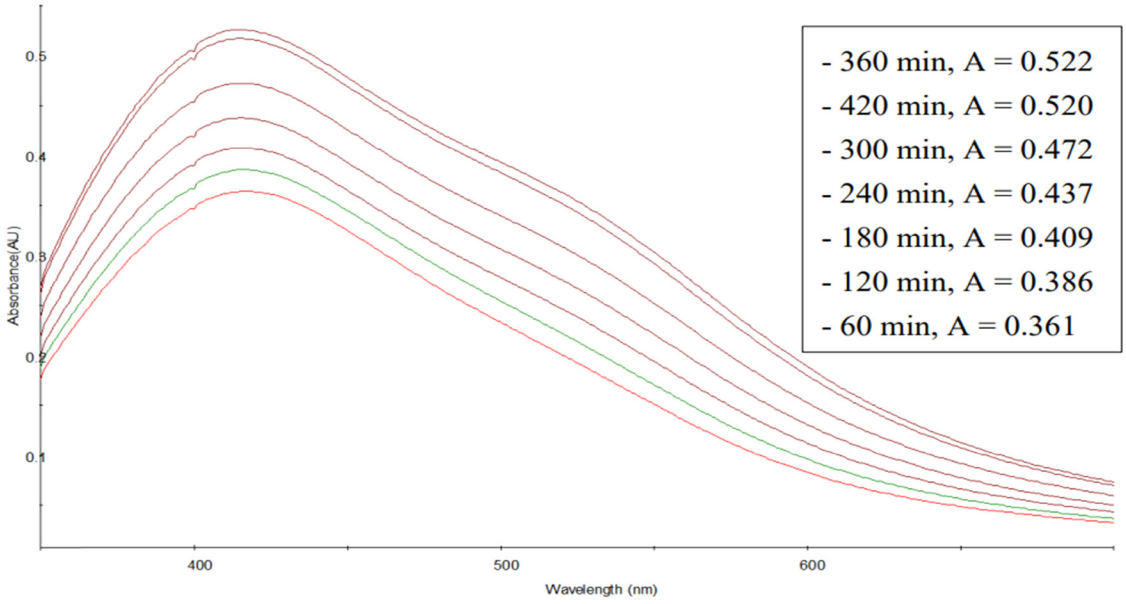

Figure 7: UV–Vis spectra of AgNPs synthesized as a function of time.

Figure 7 shows that as the reaction time of the synthesis of AgNPs increased, the measured absorption intensity value also grew. This can be explained that the longer the reaction time, the stronger the reaction of the substances in the extract with Ag^+ ions to create AgNPs, leading to a higher absorption intensity. After 360 min, the synthesis of AgNPs by *C. fragrans* leaf aqueous extract is considered complete.

In summary, the optimal conditions for the synthesis of AgNPs using *C. fragrans* leaf aqueous extract are 10 mL of extract per 30 mL of 1 mM $AgNO_3$ solution, pH 7.06, reaction temperature 80°C, and reaction time 360 min.

3.5 Field emission scanning electron microscopy (FE-SEM), TEM, EDX, and X-ray diffraction pattern (XRD) analysis of AgNPs

FE-SEM and TEM images of the produced AgNPs are shown in Figure 8. The shapes of AgNPs were spherical.

EDX spectra recorded from the AgNPs are shown in Figure 9.

X-ray diffraction pattern of AgNPs synthesized by *C. fragrans* leaf extract is shown in Figure 10. The diffraction peaks at $2\theta = 38.14°$, 44.14°, and 64.51° correspond to

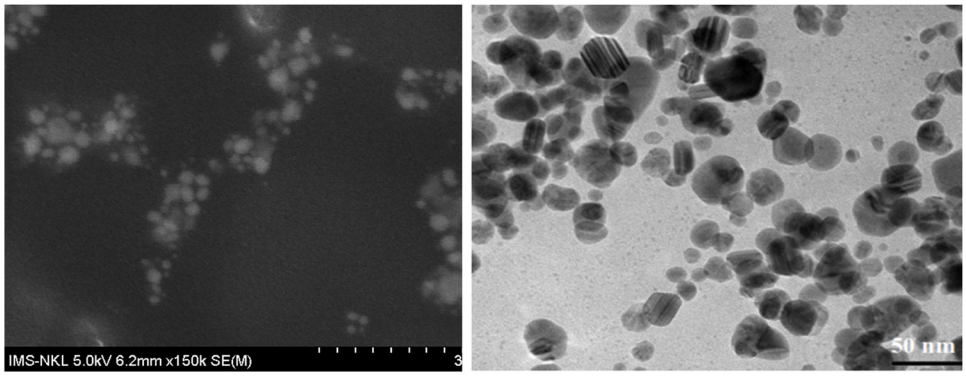

Figure 8: FE-SEM and TEM micrographs of AgNPs synthesized by aqueous extract of *C. fragrans* leaf.

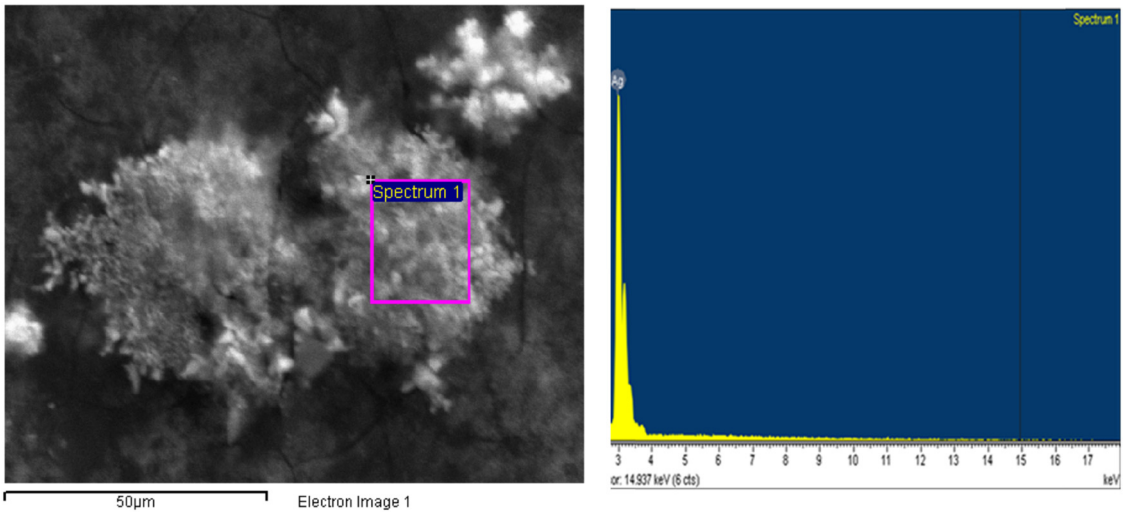

Figure 9: EDX micrograph of AgNPs synthesized by aqueous extract of *C. fragrans* leaf. The EDX spectra of the biosynthesized AgNPs show silver element, indicating that the reduction of Ag ions to AgNPs had occurred in the aqueous extract of *C. fragrans* leaf. Carbon and oxygen are also present in the EDX graph due to the organic molecules found in the extract of the *C. fragrans* leaves. These biomolecules capped the AgNPs as capping and stabilizing agents.

the (111), (200), and (220) faces of the silver fcc crystal structure, respectively.

3.6 Nanoparticle size distribution and zeta potential

The hydrodynamic diameter and size distribution of spherical AgNPs were analyzed by dynamic light scattering (DLS). Results show that the AgNPs synthesized by extract of the *C. fragrans* leaf with the average nanoparticle size was around 48.0 nm (Figure 11). The value of polydispersity index (PDI) may vary from 0.01 (mono-dispersed particles) to 0.5–0.7, whereas PDI index value >0.7 indicated broad particle size distribution of the formulation and is probably not suitable to be analyzed by the DLS technique The polydispersity index of AgNPs synthesized by the extract of the *C. fragrans* leaf was 0.523, indicating the formation of polydisperse mixture of nanoparticles [56].

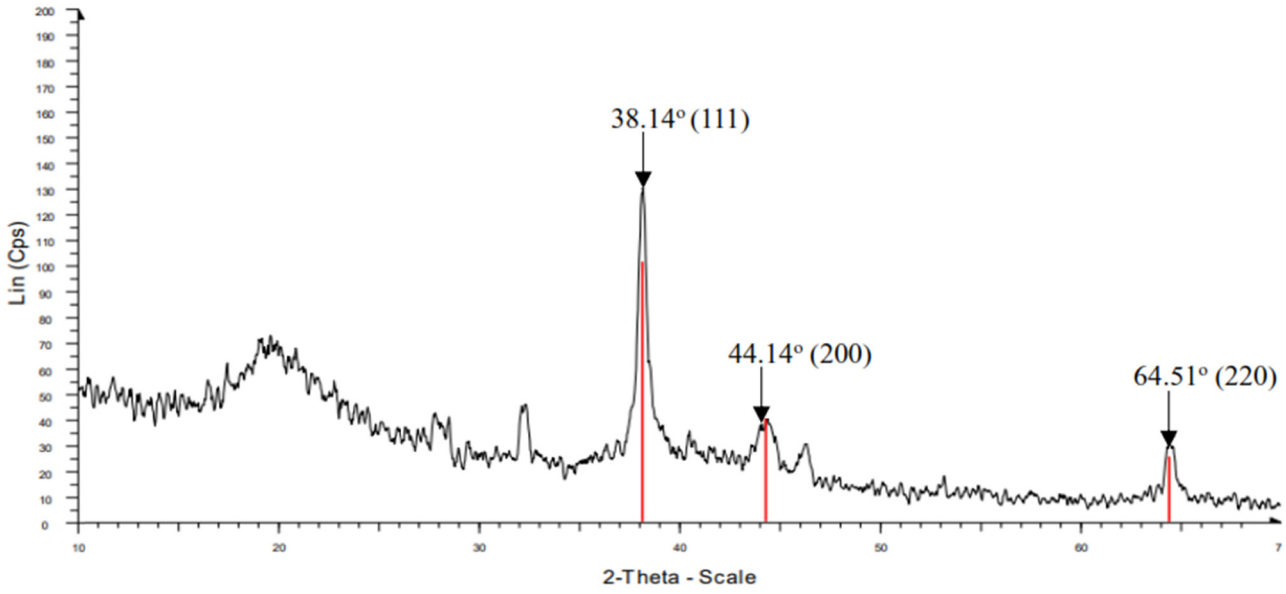

Figure 10: XRD pattern of AgNPs synthesized by *C. fragrans* leaf aqueous extract.

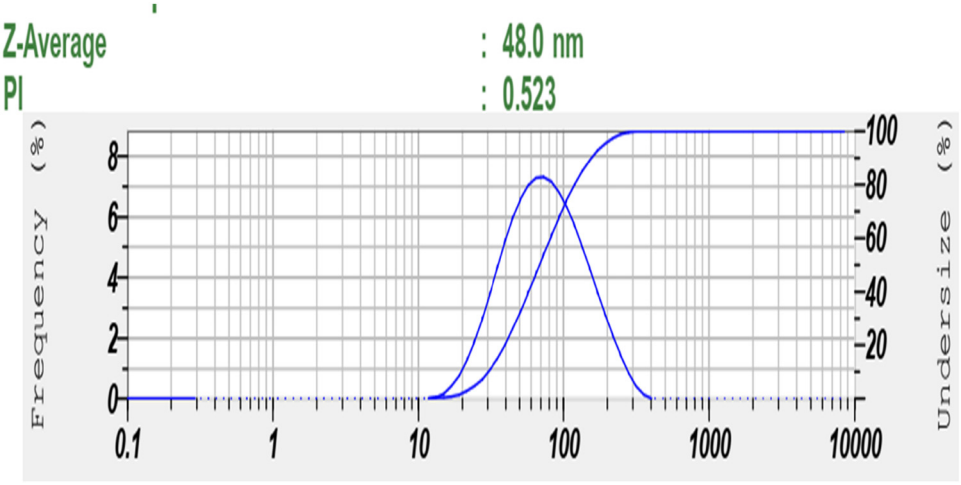

Figure 11: Size distribution mean of biosynthesized AgNPs from *C. fragrans* leaf extracts in nm.

The surface charges and stability of the nanoparticles in the suspension were measured through zeta potential and the value was about −27.0 mV (Figure 12), which indicated negative charges on the formed AgNPs. This result showed that the use of the extract of the *C. fragrans* leaf allows obtaining stable AgNPs without a stabilizer.

3.7 FTIR spectra of *C. fragrans* leaf extract and biosynthesized AgNPs

FTIR measurement was used to determine the presence of bioactive molecules that could be responsible for AgNP stabilization by acting as capping agents. The absorption spikes at 3,349.75, 2,917.77, 1,537.95, 1,385.60, and 1,076.08 cm^{-1} were determined for *C. fragrans* leaf extract, while AgNPs shows absorption spikes at 3,326.47, 2,913.91, 1,526.28, 1,329.43, and 1,014.37 cm^{-1} ((A) and (B) in Figure 13). Higher peaks at 3,349.75 and 3,326.47 cm^{-1} can be attributed to bounded hydroxyl (–OH) in alcohols in the *C. fragrans* leaf extract. The presence of smaller bands at 2,917.77 and 2,913.91 cm^{-1} for extract and AgNPs was due to the –CH stretching in alkanes. Peaks at 1,537.95 cm^{-1} (extract) and 1,526.28 cm^{-1} (AgNPs) correspond to the C═O group. The bands at 1,385.60 cm^{-1} (extract) and 1,329.43 cm^{-1} (AgNPs) correspond to the C–O–C group. The peaks at 1,076 cm^{-1} (extract) and 1,014 cm^{-1} (AgNPs) are attributed to the C–O stretching in esters that were found in the leaf extract. The spectrum of AgNPs ((B) in Figure 13) was observed to be

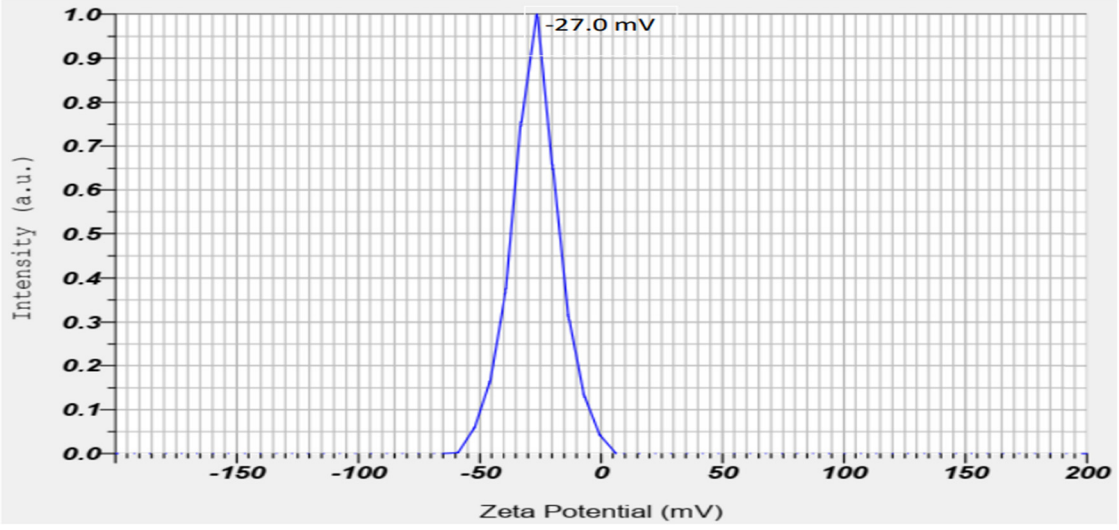

Figure 12: Zeta potential of AgNPs from *C. fragrans* leaf extracts in mV.

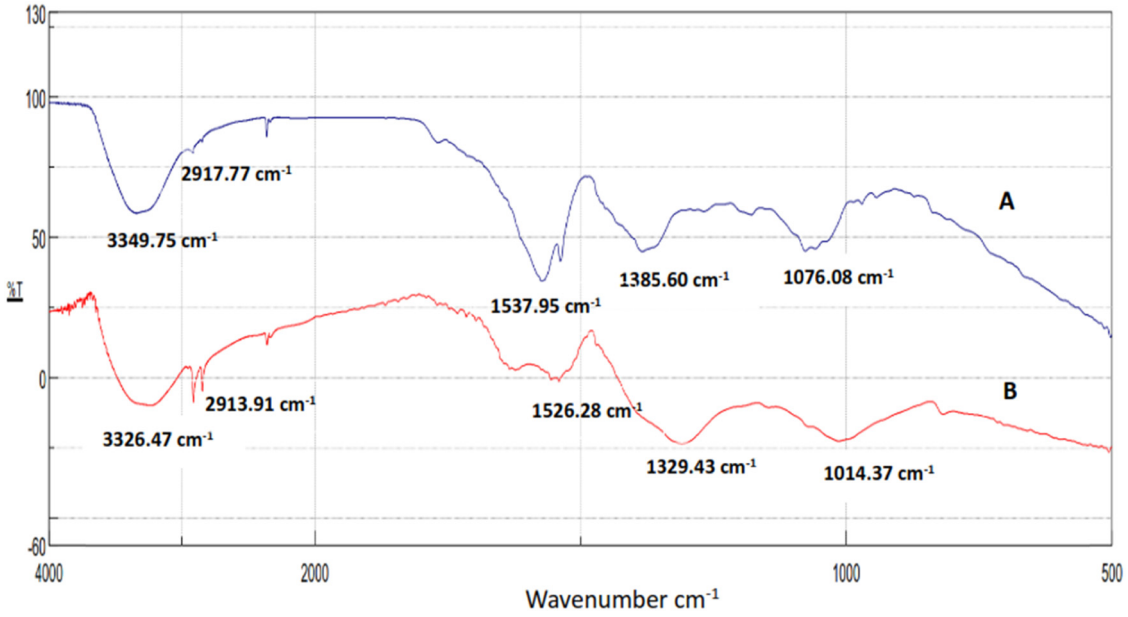

Figure 13: FTIR spectra of *C. fragrans* leaf extracts (A) and AgNPs biosynthesized using the leaf extracts (B).

similar to (A) in Figure 13 regarding the sites of the functional groups. Therefore, these groups found in plant leaf extracts were responsible for silver nitrate reduction to AgNPs and capping nanoparticles for stabilization and preventing their aggregation in the medium.

3.8 Mechanism of the formation of AgNPs by aqueous extract of *C. fragrans* leaf

Based on the results of phytochemical screening and determination of chemical compositions by GC–MS, the

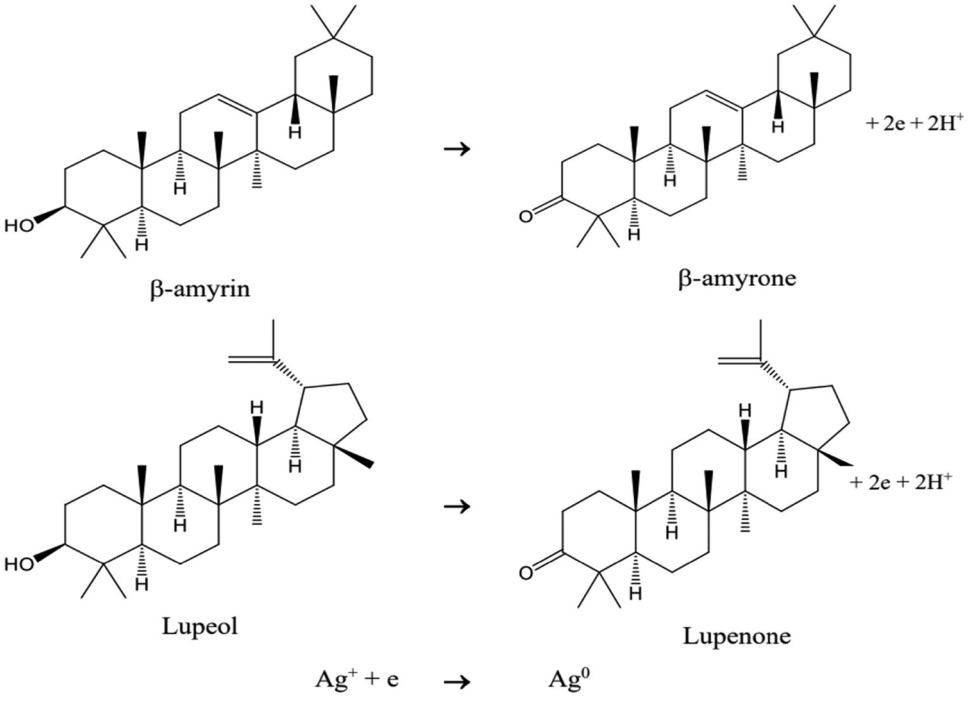

Figure 14: Mechanism of reduction of Ag^+ to Ag^0 by *C. fragrans* leaf extract.

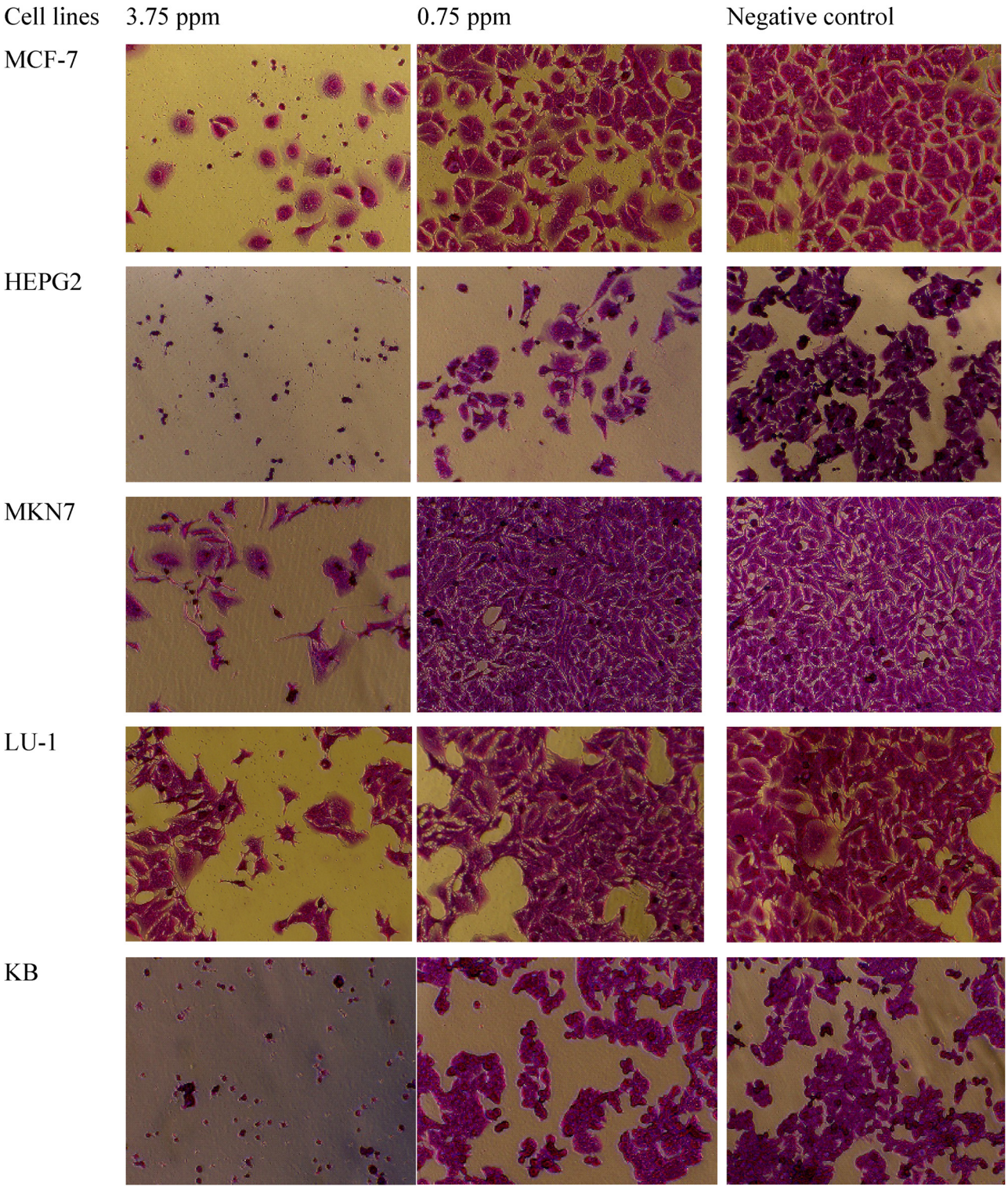

Figure 15: Anticancer activity of *C. fragrans* leaf AgNPs against MCF-7, HepG2, MKN7, LU-1, and KB cell lines (the magnification in microscopic images is 20×).

aqueous extract of *C. fragrans* leaf contains functional groups of terpenoids, flavonoids, tannin, and saponin; these groups of substances will act as the reducing agent Ag^{+} to Ag [57,58]. In particular, the presence of β-amyrin and lupeol with the –OH group in the ring may undergo oxidation and get converted to quinone forms of β-amyrone

Table 3: *In vitro* cytotoxicity effect of AgNPs from the *C. fragrans* leaf on cancer cell lines represented as cell inhibition percentage ± standard deviation

Concentration (ppm)	MCF-7		HepG2		KB		LU-1		MKN-7	
	% of inhibition	SD	% of inhibition	SD	% of inhibition	SD	% of inhibition	SD	% of inhibition	SD
3.75	79.40	2.78	82.57	2.55	75.64	3.73	62.95	3.10	80.81	2.13
0.75	14.74	1.49	16.41	0.16	11.30	1.40	7.04	0.63	13.02	1.13
0.15	5.95	0.48	7.25	0.27	1.90	0.16	3.73	0.44	1.80	0.48
0.03	0.21	0.05	2.06	0.36	0.65	0.17	3.47	0.26	−1.98	0.81
IC_{50}	**2.41 ± 0.23**		**2.31 ± 0.25**		**2.65 ± 0.39**		**3.26 ± 0.28**		**2.40 ± 0.33**	

SD = standard deviation.

and lupenone, respectively. The synthesized AgNPs are stabilized through the lone pair of electrons and p electrons of quinone structures of lupenone and β-amyrone and other organic compounds in the aqueous extract of *C. fragrans* leaves (Figure 14).

Figure 14 shows that, when the pH level of the solution is low, the oxidation reactions of β-amyrin and lupeol are not favored, so the ability to reduce Ag^+ into Ag decreases. When the pH of the solution increases, the equilibrium of the oxidation reaction of β-amyrin and lupeol shifts from rightward, raising the rate of the reduction reaction $Ag^+ \rightarrow Ag$ and the amount of synthesized AgNPs. This reaction mechanism is consistent with the results produced from investigating the effect of pH on the synthesis of AgNPs.

3.9 Anticancer activity

The viability of MCF-7 (human breast carcinoma), LU-1 (human lung carcinoma), HepG2 (human hepatocellular carcinoma), KB (human carcinoma in the mouth), and MKN-7 (human gastric carcinoma) cancer cells with AgNPs for 72 h was determined using the colorimetric SRB assay.

The obtained results showed that MCF-7 cells proliferation was significantly inhibited by AgNPs with an IC_{50} value of 2.41 $\mu g \cdot mL^{-1}$, HepG2 cells with an IC_{50} value of 2.31 $\mu g \cdot mL^{-1}$, KB cells with an IC_{50} value of 2.65 $\mu g \cdot mL^{-1}$, LU-1 cells with an IC_{50} value of 3.26 $\mu g \cdot mL^{-1}$ of the concentration and MKN-7 cells with an IC_{50} value of 2.40 $\mu g \cdot mL^{-1}$. The cytotoxicity of metal nanomaterials is associated with the various parameters such as sizes, morphologies, and surface charges as well as different biological resources that act as reducing and capping agents [59–61]. The IC_{50} values (2.41 and 2.31 $\mu g \cdot mL^{-1}$) for MCF-7 and HepG2 cancer cell lines of AgNPs synthesized from the aqueous extract of *C. fragrans* leaves are low compared to the IC_{50} values of AgNPs synthesized from other plant extracts [62–64]. The reason is that extracts of *C. fragrans* leaves contain beta-amyrin and lupeol. These substances participate in a redox reaction with Ag^+ ions to convert to beta-amyrone and lupenone, which are active substances with excellent anticancer properties [65,66]. The presence of these substances on the surface of AgNPs has significantly increased the anticancer ability of AgNPs. Thus, AgNPs were synthesized in this study and showed good anticancer activity against MCF-7, HepG2, KB, LU-1, and MKN-7 cell lines (Figure 15, Table 3).

4 Conclusions

The bio-reduction of Ag^+ ion using the aqueous extract of *C. fragrans* leaves leading to the formation of AgNPs of fairly well-defined dimensions has been demonstrated to have the optimal conditions of 10 mL of extract (15 g of *C. fragrans* leaf per 100 mL of water, extraction time 70 min, boiling temperature) per 30 mL of 1 mM $AgNO_3$, temperature 80°C, pH = 7.06, reaction time 360 min. XRD result shows the face-centered cubic lattice of AgNPs. The synthesized AgNPs are mostly spherical in shape with an average size of 48.0 nm. The zeta potential of AgNPs is −27.0 mV. The aqueous extract of *C. fragrans* leaf acts as a reducing and stabilizing agent. The synthesis of AgNPs using *C. fragrans* leaf extract holds the environmental advantage over alternative chemical synthesis methods due to the absence of pollutants produced. Promisingly, the synthesized AgNPs demonstrated anticancer activity against MCF-7, HepG2, KB, LU-1, and MKN-7 cell lines. This study thus demonstrates that synthesizing AgNPs by using aqueous extract of *C. fragrans* not only generates considerably lower environmental impacts, but the resulting product also possesses incredible potential as life-saving anticancer agents.

Funding information: The authors would like to acknowledge the financial support provided by The Ministry of Education and Training of Vietnam under the grant number B2022-DNA-05.

Author contributions: Lan Anh Thi Nguyen: conceived and designed the analysis, collected the data, contributed data or analysis tools, and performed the analysis; Bay Van Mai: conceived and designed the analysis, collected the data, contributed data or analysis tools, and performed the analysis; Din Van Nguyen: conceived and designed the analysis and performed the analysis; Ngoc Quyen Thi Nguyen: conceived and designed the analysis, collected the data, contributed data or analysis tools, and performed the analysis; Vuong Van Pham: conceived and designed the analysis and performed the analysis; Thong Le Minh Pham: conceived and designed the analysis, collected the data, performed the analysis, and writing – original draft; Hai Tu Le: conceived and designed the analysis, collected the data, performed the analysis, and writing – original draft, writing – review and editing.

Conflict of interest: The authors state no conflict of interest.

References

[1] Joudeh N, Linke D. Nanoparticle classification, physicochemical properties, characterization, and applications: a comprehensive review for biologists. J Nanobiotechnol. 2022;20:262. doi: 10.1186/s12951-022-01477-8.

[2] Sharma A, Goyal AK, Rath G. Recent advances in metal nanoparticles in cancer therapy. J Drug Target. 2018;8:617–32. doi: 10.1080/1061186X.2017.1400553.

[3] Barabad H. Nanobiotechnology: a promising scope of gold biotechnology. Cell Mol Biol. 2017;63(12):3–4. doi: 10.14715/cmb/2017.63.12.2.

[4] Vahidi H, Kobarfard F, Alizadeh A, Saravanan M, Barabadi H. Green nanotechnology-based tellurium nanoparticles: exploration of their antioxidant, antibacterial, antifungal and cytotoxic potentials against cancerous and normal cells compared to potassium tellurite. Inorg Chem Commun. 2021;124:108385.

[5] Cruz MD, Mostafavi E, Vernet-Crua A, Barabadi H, Cholula-Díaz LJ, Guisbiers G, et al. Green nanotechnology-based zinc oxide (ZnO) nanomaterials for biomedical applications: a review. J Phys Mater. 2020;3:034005.

[6] Burdusel AC, Gherasim O, Grumezescu AM, Mogoantă L, Ficai A, Andronescu E. Biomedical applications of silver nanoparticles: an up-to-date overview. Nanomaterials. 2018;8:681.

[7] Chaloupka K, Malam Y, Seifalian AM. Nanosilver as a new generation of nanoproduct in biomedical applications. Trends Biotechnol. 2010;28(11):580–8.

[8] Viana RLS, Fidelis GP, Medeiros JC, Morgano MA, Alves MG, Passero LFD, et al. Green synthesis of antileishmanial and antifungal silvernanoparticles using Corn Cob Xylan as a reducing and stabilizing agent. Biomolecules. 2020;10:1235.

[9] Zulkifli NI, Muhamad M, Zain NNM, Tan WN, Yahaya N, Bustami Y, et al. A bottom-up synthesis approach to silver nanoparticles induces anti-proliferative and apoptotic activities against MCF-7, MCF-7/TAMR-1 and MCF-10A human breast cell lines. Molecules. 2020;25:4332. doi: 10.3390/molecules25184332

[10] Kaur J, Tikoo K. Evaluating cell specific cytotoxicity of differentially charged silver nanoparticles. Food Chem Toxicol. 2013;51(1):1–14.

[11] Sufyani NMA, Hussien NA, Hawsawi YM. Characterization and anticancer potential of silver nanoparticles biosynthesized from *Olea chrysophylla* and *Lavandula dentata* leaf extracts on HCT116 colon cancer cells. J Nanomater. 2019;2019:7361695.

[12] Paul JA, Selvi BK, Karmegam N. Biosynthesis of silver nanoparticles from *Premna serratifolia* L. leaf and its anticancer activity in CCl_4-induced hepato-cancerous Swiss albino mice. Appl Nanosci. 2015;5:937–44.

[13] Velammal PS, Devi AT, Amaladhas PT. Antioxidant, antimicrobial and cytotoxic activities of silver and gold nanoparticles synthesized using *Plumbago zeylanica* bark. J Nanostruct Chem. 2016;6:247–60. doi: 10.1007/s40097-016-0198-x.

[14] Hawar SN, Al-Shmgani HS, Al-Kubaisi ZA, Sulaiman GM, Dewir YH, Rikisahedew JJ. Green synthesis of silver nanoparticles from *Alhagi graecorum* leaf extract and evaluation of their cytotoxicity and antifungal activity. J Nanomater. 2022;2022:8. doi: 10.1155/2022/1058119.

[15] Younas M, Rizwan M, Zubair M, Inam A, Ali S. Biological synthesis, characterization of three metal-based nanoparticles and their anticancer activities against hepatocellular carcinoma HepG2 cells. Ecotoxicol Environ Saf. 2021;223:112575.

[16] Walimbe KG, Dhawal PP, Kakodkar SA. Anticancer potential of biosynthesized silver nanoparticles: a review. Eur J Biol Biotechnol. 2022;3(2):10–20. doi: 10.24018/ejbio.2022.3.2.338.

[17] Tadele KT, Abire TO, Feyisa TY. Green synthesized silver nanoparticles using plant extracts as promising prospect for cancer therapy: a review of recent findings. J Nanomed. 2021;4(1):1040.

[18] Oves M, Rauf MA, Aslam M, Qari HA, Sonbol H, Ahmad I, et al. Green synthesis of silver nanoparticles by *Conocarpus lancifolius* plant extract and their antimicrobial and anticancer activities. Saudi J Biol Sci. 2022;29:460–71.

[19] Matteis VD, Cascione M, Toma CC, Leporatti S. Silver nanoparticles: synthetic routes, in vitro toxicity and theranostic applications for cancer disease. Nanomaterials. 2018;8:319. doi: 10.3390/nano8050319.

[20] Gurunathan S, Raman J, Malek ANS, John AP, Vikineswary S. Green synthesis of silver nanoparticles using *Ganoderma neojaponicum* Imazeki: a potential cytotoxic agent against breast cancer cells. Int J Nanomed. 2013;8:4399–413.

[21] Mafune F, Kohno J, Takeda Y, Kondow T, Sawabe H. Structure and stability of silver nanoparticles in aqueous solution produced by laser ablation. J Phys Chem B. 2000;104(35):8333–7.

[22] Tien CD, Lao Y, Huang CJ, Tseng HK, Lung KJ, Tsung TT, et al. Novel technique for preparing a nano-silverswater suspension by the arc discharge method. Rev Adv Mater Sci. 2008;18:750–6.

[23] Pingali CK, Rockstraw AD, Deng S. Silver nanoparticles from ultrasonic spray pyrolysis of aqueous silver nitrate. Aerosol Sci Technol. 2005;39:1010–4.
[24] Haider JM, Mahdi SM. Synthesis of silver nanoparticles by electrochemical method. Eng Tech J. 2015;33(7)Part (B):1361–73.
[25] Quintero-Quiroz C, Acevedo N, Zapata-Giraldo J, Botero EL, Quintero J, Zárate-Triviño D, et al. Optimization of silver nanoparticle synthesis by chemical reduction and evaluation of its antimicrobial and toxic activity. Biomater Res. 2019;23:27. doi: 10.1186/s40824-019-0173-y.
[26] Chen P, Song L, Liu Y, Fang Y. Synthesis of silver nanoparticles by γ-ray irradiation in acetic water solution containing chitosan. Radiat Phys Chem. 2007;76(7):1165–8.
[27] Pryshchepa O, Pomastowski, P, Buszewski, B. Silver nanoparticles: synthesis, investigation techniques, and properties. Adv Colloid Interface Sci. 2020;284:102246.
[28] Rahimirad A, Javadi A, Mirzaei H, Anarjan N, Jafarizadeh-Malmiri H. Biosynthetic potential assessment of four food pathogenic bacteria in hydrothermally silver nanoparticles fabrication. Green Process Synth. 2019;8:629–34. doi: 10.1515/gps-2019-0033
[29] Mukherjee P, Ahmad A, Mandal D, Senapati S, Sainkar RS, Khan IM, et al. Fungus-mediated synthesis of silver nanoparticles and their immobilization in the mycelial matrix: a novel biological approach to nanoparticle synthesis. Nano Lett. 2001;1(10):515–9.
[30] Chugh D, Viswamalya SV, Das B. Green synthesis of silver nanoparticles with algae and the importance of capping agents in the process. J Genet Eng Biotechnol. 2021;19:126.
[31] Niknejad F, Nabili M, Daie Ghazvini R, Moazeni M. Green synthesis of silver nanoparticles: advantages of the yeast *Saccharomyces cerevisiae* model. Curr Med Mycol. 2015;1(3):17–24. doi: 10.18869/acadpub.cmm.1.3.17.
[32] Torabfam M, Jafarizadeh-Malmiri H. Microwave-enhanced silver nanoparticle synthesis using chitosan biopolymer: optimization of the process conditions and evaluation of their characteristics. Green Process Synth. 2018;7:530–7. doi: 10.1515/gps-2017-0139.
[33] Varadharaj V, Ramaswamy A, Sakthivel R, Subbaiya R, Barabadi H, Chandrasekaran M, et al. Antidiabetic and antioxidant activity of green synthesized starch nanoparticles: an in vitro study. J Clust Sci. 2020;31:1257–66. doi: 10.1007/s10876-019-01732-3.
[34] Rafique M, Sadaf I, Rafique MS, Tahir MB. A review on green synthesis of silver nanoparticles and their applications. Artif Cells Nanomed Biotechnol. 2017;45(7):1272–91.
[35] Abdelghany TM, Al-Rajhi AMH, Al Abboud MA, Alawlaqi MM, Magdah AG, Helmy EAM, et al. Recent advances in green synthesis of silver nanoparticles and their applications: about future directions. A review. BioNanoScience. 2018;8:5–16.
[36] Tarannum N, Divya, Gautam YK. Facile green synthesis and applications of silver nanoparticles: a state-of-the-art review. RSC Adv. 2019;9:34926–48.
[37] Vanlalveni C, Lallianrawna S, Biswas A, Selvaraj M, Changmai B, Rokhum SL. Green synthesis of silver nanoparticles using plant extracts and their antimicrobial activities: a review of recent literature. RSC Adv. 2021;11:2804–37.
[38] Zargar M, Hamid AA, Bakar FA, Shamsudin MN, Shameli K, Jahanshiri F, et al. Green synthesis and antibacterial effect of silver nanoparticles using *Vitex negundo* L. Molecules. 2011;16:6667–76.
[39] Masurkar SA, Chaudhari PR, Shidore VB, Kamble SP. Rapid biosynthesis of silver nanoparticles using *Cymbopogan citratus* (lemongrass) and its antimicrobial activity. Nano-Micro Lett. 2011;3:189–94.
[40] Ahmadi O, Jafarizadeh-Malmiri H, Jodeiri N. Eco-friendly microwave-enhanced green synthesis of silver nanoparticles using *Aloe vera* leaf extract and their physico-chemical and antibacterial studies. Green Process Synth. 2018;7:231–40. doi: 10.1515/gps-2017-0039.
[41] Ghanbari S, Vaghari H, Sayyar Z, Adibpour M, Jafarizadeh-Malmiri H. Autoclave-assisted green synthesis of silver nanoparticles using *A. fumigatus* mycelia extract and the evaluation of their physico-chemical properties and antibacterial activity. Green Process Synth. 2018;7:217–24. doi: 10.1515/gps-2017-0062.
[42] Eshghi M, Kamali-Shojaei A, Vaghari H, Najian Y, Mohebian Z, Ahmadi O, et al. *Corylus avellana* leaf extract-mediated green synthesis of antifungal silver nanoparticles using microwave irradiation and assessment of their properties. Green Process Synth. 2021;10:606–13. doi: 10.1515/gps-2021-0062.
[43] Rai M, Posten C. Green biosynthesis of nanoparticles mechanisms and applications. Printed and Bound in the UK by Berforts Information Press Ltd; 2013.
[44] Chernenko TV, Ul'chenko NT, Glushenkova AI, Redzhepov D. Chemical investigation of *Callisia fragrans*. Chem Nat Compd. 2007;43:253–5.
[45] Olennikov DN, Nazarova AV, Rokhin AV, Ibragimov TA, Zilfikarov IN. Chemical composition of *Callisia fragrans* juice. II. Carbohydrates. Chem Nat Compd. 2010;46:273–5.
[46] Sohafy SM, Nassra RA, D'Urso G, Piacente S, Sallam SM. Chemical profiling and biological screening with potential anti-inflammatory activity of *Callisia fragrans* grown in Egypt. Nat Product Res. 2021;35:5521–4.
[47] Soni A, Sosa S. Phytochemical analysis and free radical scavenging potential of herbal and medicinal plant extracts. J Pharmacogn Phytochem. 2013;2(4):22–9.
[48] Nagar N, Jain S, Kachhawah P, Devra V. Synthesis and characterization of silver nanoparticles via green route. Korean J Chem Eng. 2016;33(10):2990–7.
[49] Mittal AK, Kaler A, Banerjee UC. Free radical scavenging and antioxidant activity of silver nanoparticles synthesized from flower extract of *Rhododendron dauricum*. Nano Biomed Eng. 2012;4(3):118–24.
[50] Dubey SP, Lahtinen M, Sillanpää M. Tansy fruit mediated greener synthesis of silver and gold nanoparticles. Process Biochem. 2010;45:1065–71.
[51] Heydari R, Rashidipour M. Green synthesis of silver nanoparticles using extract of oak fruit hull (Jaft): synthesis and in vitro cytotoxic effect on MCF-7cells. Int J Breast Cancer. 2015;6:1–6. doi: 10.1155/2015/846743.
[52] Iravani S, Zolfaghari B. Green synthesis of silver nanoparticles using *Pinus eldarica* bark extract. BioMed Res Int. 2013;2013:5. Article ID 639725. doi: 10.1155/2013/639725.
[53] Melkamu WW, Bitew TL. Green synthesis of silver nanoparticles using *Hagenia abyssinica* (*Bruce*) *J.F.Gmel* plant leaf extract and their antibacterial and anti-oxidant activities. Heliyon. 2021;7:e08459.

[54] Heydari R. Biological applications of biosynthesized silver nanoparticles through the utilization of plant extracts. Herb Med J. 2017;2(2):87–95.
[55] Sarsar V, Selwal KM, Selwel KK. Significant parameters in the optimization of biosysnthesis o silver nanoparticles using *Psidium guajava* leaf extract and evaluation of their antimicrobial activity against human pathogenic bacteria. Int J Adv Pharma Sci. 2014;5(1):1769–75.
[56] Nidhin M, Indumathy R, Sreeram JK, Nair BU. Synthesis of iron oxide nanoparticles of narrow size distribution on polysaccharide templates. Bull Mater Sci. 2008;31(1):93–6.
[57] Ullah I, Khalil AT, Ali M, Iqbal J, Ali W, Alarifi S, et al. Green-synthesized silver nanoparticles induced apoptotic cell death in MCF-7 breast cancer cells by generating reactive oxygen species and activating caspase 3 and 9 enzyme activities. Oxid Med Cell Longev. 2020;2020:1215395.
[58] Mashwani ZR, Khan MA, Khan T. Applications of plant terpenoids in the synthesis of colloidal silver nanoparticles. Adv Colloid Interface Sci. 2016;234:132–41.
[59] Mostafavi E, Zarepour A, Barabadi H, Zarrabi A, Truong BL, Medina-Cruz D. Antineoplastic activity of biogenic silver and gold nanoparticles to combat leukemia: beginning a new era in cancer theragnostic. Biotechnol Rep. 2022;34:e00714.
[60] Virmani I, Sasi C, Priyadarshini E, Kumar R, Sharma KS, Singh PG, et al. Comparative anticancer potential of biologically and chemically synthesized gold nanoparticles. J Clust Sci. 2020;31:867–76. doi: 10.1007/s10876-019-01695-5.
[61] Barabadi H, Vahidi H, Mahjoub AM, Kosar Z, Kamali DK, Ponmurugan K, et al. Emerging antineoplastic gold nanomaterials for cervical cancer therapeutics: a systematic review. J Clust Sci. 2020;31:1173–84. doi: 10.1007/s10876-019-01733-2.
[62] Alahmad A, Feldhoff A, Bigall NC, Rusch P, Scheper T. *Hypericum perforatum* L.-mediated green synthesis of silver nanoparticles exhibiting antioxidant and anticancer activities. Nanomaterials. 2021;11:487.
[63] Patra JK, Das G, Shin HS. Facile green biosynthesis of silver nanoparticles using *Pisum sativum* L. outer peel aqueous extract and its antidiabetic, cytotoxicity, antioxidant, and antibacterial activity. Int J Nanomed. 2019;14:6679–90.
[64] Hashemi Z, Mizwari ZM, Mohammadi-Aghdam S, Mortazavi-Derazkola S, Ebrahimzadeh MA. Sustainable green synthesis of silver nanoparticles using *Sambucus ebulus* phenolic extract (AgNPs@SEE): optimization and assessment of photocatalytic degradation of methyl orange and their in vitro antibacterial and anticancer activity. Arab J Chem. 2022;15:103525.
[65] Almeida PDO, Boleti APA, Rüdiger AL, Lourenço GA, Veiga Junior VF, Lima ES. Anti-inflammatory activity of triterpenes isolated from protium paniculatum oil-resins. Evid-Based Complementary Altern Med. 2015;10:Article ID 293768.
[66] Ferreira RGS, Silva Júnior WF, Veiga Junior VF, Lima AAN, Lima ES. Physicochemical characterization and biological activities of the triterpenic mixture α, β-amyrenone. Molecules. 2017;22:298. doi: 10.3390/molecules22020298.